https://doi.org/10.5194/egusphere-2024-2776
Preprint. Discussion started: 25 November 2024

Technical note: Reconstructing surface missing aerosol elemental carbon data in long-term series with ensemble learning

Qingxiao Meng[1], Yunjiang Zhang[1*], Sheng Zhong[2], Jie Fang[1], Lili Tang[3], Yongcai Rao[4], Minfeng Zhou[5], Jian Qiu[6], Xiaofeng Xu[7], Jean-Eudes Petit[8], Olivier Favez[9], Xinlei Ge[1]

[1]Collaborative Innovation Center of Atmospheric Environment and Equipment Technology, Jiangsu Key Laboratory of Atmospheric Environment Monitoring and Pollution Control, School of Environmental Science and Engineering, Nanjing University of Information Science and Technology, Nanjing 210044, China
[2]Jiangsu Environmental Monitoring Center, Nanjing, China
[3]Nanjing Rayleigh Scientific Instruments Co., Ltd., Nanjing, China
[4]Xuzhou Environmental Monitoring Center of Jiangsu, Xuzhou, China
[5]Suzhou Environmental Monitoring Center of Jiangsu, Suzhou, China
[6]Zhenjiang Environmental Monitoring Center of Jiangsu, Zhenjiang, China
[7]Key Laboratory for Aerosol-Cloud-Precipitation of China Meteorological Administration, School of Atmospheric Physics, Nanjing University of Information Science and Technology, Nanjing 210044, China
[8]Laboratoire des Sciences du Climat et de l'Environnement, CEA/Orme des Merisiers, Gif sur Yvette, France
[9]Institut National de l'Environnement Industriel et des Risques, Verneuil-en-Halatte, France

Correspondence to: Yunjiang Zhang (yjzhang@nuist.edu.cn)

Abstract. Ground-based measurements of elemental carbon (EC) – classified under thermal-optical methods and considered as a surrogate for black carbon – are essential for assessing air quality and evaluating climate impacts. However, data gaps caused by technical challenges impede comprehensive analyses of long-term trends. This study proposes an ensemble learning method to address these challenges. The model uses readily accessible ground observation air pollutant data as proxies for EC-related tracers, along with meteorological parameters, to enhance prediction accuracy. It integrates outputs from Gradient Boosting Regression Trees, eXtreme Gradient Boosting, and Random Forest models, combining them through ridge regression to produce robust predictions. We applied this approach to reconstruct hourly EC concentrations from 2013 to 2023 for four cities in Eastern China, filling 45-79% of missing data and improving prediction performance by 8-17% compared to individual models. Over the 11-year period, EC exhibited an overall decline (-0.20 to -0.14 μg m^{-3} a^{-1}), with a more significant decline from 2013 to 2020 (-0.24 to -0.15 μg m^{-3} a^{-1}) from 3.26 μg m^{-3} to 1.59 μg m^{-3}, followed by a noticeable slowdown from 2020 to 2023 (-0.12 to -0.04 μg m^{-3} a^{-1}). Additionally, a fixed emission approximation method based on ensemble learning is proposed to quantitatively analyze the drivers of long-term EC trends. The analysis reveals that anthropogenic emission

https://doi.org/10.5194/egusphere-2024-2776
Preprint. Discussion started: 25 November 2024

controls were the predominant contributors, accounting for approximately 92 % of the changes in EC trends from 2013 to 2020. However, their influence weakened post-2020, contributing approximately 80 %. These findings highlight that while China's Clean Air Actions implemented since 2013 have significantly reduced black carbon concentrations, sustained and enhanced strategies are still necessary to further mitigate black carbon pollution in the country.

1 Introduction

Black carbon (BC), derived from the incomplete combustion of fossil or biomass fuels (Bond & Bergstrom, 2006), is a significant component of fine particulate matter ($PM_{2.5}$) in the troposphere. BC has a strong capacity to absorb visible light (Bond et al., 2013), which can directly or indirectly affect global climate change (Ramanathan & Carmichael, 2008) and influence the structure of the urban boundary layer, exacerbating regional air pollution formation (Ding et al., 2016). Additionally, BC particles, which are small in size and rich in toxic substances on their surfaces, pose significant health risks (Valavanidis et al., 2013), leading to respiratory and cardiovascular diseases (Wei et al., 2023). Therefore, establishing long-term trends of BC is crucial for studying its climate, environmental, and health impacts.

Methods for determining ground-level BC concentrations and long-term trends generally include ground-based in-situ observations (Peng et al., 2019; Wei et al., 2020), satellite retrievals (Yu et al., 2024; Zhao et al., 2021), and atmospheric chemical transport model simulations (Yang et al., 2021). Satellite-based retrieval methods are often used to characterize ground-level BC concentrations. For instance, Li et al. (2022) used multi-angle polarization satellite observations to retrieve the spatiotemporal distribution of global BC concentrations. However, satellite data are susceptible to noise originating from clouds and other factors, leading to data gaps and large uncertainties (Bao et al., 2019; Zhao et al., 2021). For example, Gogoi et al. (2023) compared in-situ BC observations in India from 2019 to 2020 with BC concentrations retrieved by the Cloud and Aerosol Imager-2 (CAI-2) onboard the Greenhouse gases Observing Satellite-2 (GOSAT-2) and found a 33% bias. Beyond measurement uncertainties, satellite retrieval techniques also generally cannot provide long-term, continuous high-time-resolution (e.g., hourly) datasets.

To address the limitations of satellite retrievals, reanalysis datasets have developed, combining various in-situ, satellite observations, and short-term numerical weather prediction products through data reanalysis techniques. Notable datasets include the ECMWF Re-Analysis Interim (ERA-Interim) (Dee et al., 2011), MODIS Atmosphere and Land Reanalysis (MODIS) (Levy et al., 2013), and Modern-Era Retrospective Analysis for Research and Applications, version 2 (MERRA-2) (Randles et al., 2017). MERRA-2, in particular, offers convenient high-time-resolution datasets for atmospheric pollutants, including BC (Bali et al., 2017). However, there are uncertainties when comparing ground-based observations to reanalysis data. For instance, several studies found that MERRA-2 overestimated BC concentrations at most Chinese stations by approximately 30% (Ma et al., 2021; Xu et al., 2020; Yu et al., 2024). Atmospheric chemical transport models are also commonly used to simulate the spatiotemporal distribution of BC concentrations. For example, Matsui (2020) et al. used the Community Atmosphere Model Version 5 (CAM5) and the Aerosol Two-dimensional bin module for foRmation and Aging

https://doi.org/10.5194/egusphere-2024-2776
Preprint. Discussion started: 25 November 2024

Simulation (ATRAS) model to simulate the increase in global BC concentrations from pre-industrial times to the present. However, uncertainties in parameterization schemes for some physical and chemical processes in numerical models remain (Ervens, 2015; Harrison, 2018). Additionally, emission inventories used in models have inherent uncertainties and may not be updated promptly, affecting simulation results (Xu et al., 2021).

In situ observations remain the most direct and effective method for quantifying BC concentrations. In practice, elemental carbon (EC), measured using thermal-optical methods, is often employed as a surrogate for BC (Bond et al., 2013), especially in cases where optical methods are unavailable. These ground-based measurements (EC and/or BC) are central to long-term observational networks worldwide, such as the Atmospheric Science and Chemistry Measurement Network (ASCENT) in the United States (Ng et al., 2022), the Aerosol, Clouds, and Trace Gases Research Infrastructure (ACTRIS) in Europe (Laj et al., 2024), and the China Atmosphere Watch Network (CAWNET) in China (Zhang et al., 2014). While these methods enable the establishment of time series for BC or EC concentrations, they lack the capacity to provide historical data without prior measurements. Furthermore, practical challenges such as instrument malfunctions, routine maintenance, and hardware limitations at observation sites often lead to data gaps. These interruptions hinder the continuity and completeness of long-term datasets, posing significant challenges for trend analysis and comprehensive assessments.

This study introduces an ensemble learning method leveraging ground-based observational data (including in-situ EC and air pollutant measurements), BC column concentration assimilation data, and meteorological datasets. Applying this approach, we successfully reconstructed hourly EC concentration time series for four representative cities in the Yangtze River Delta region in Eastern China from 2013 to 2023. Furthermore, an ensemble learning model was developed to evaluate the drivers of EC trends, enabling a quantitative analysis of the relative contributions of anthropogenic emission reductions and meteorological variations to the EC trends in these cities over the 11-year period.

2 Data and Methods

2.1 Air pollutant and metrological data

The observation sites for this study are located in the representative cities of Nanjing, Suzhou, Xuzhou, and Zhenjiang within the Yangtze River Delta city cluster in Eastern China. All these sites are urban monitoring stations, and the coordinates of the sampling points are provided in Table S1. Gaseous pollutants at the corresponding sites in the four cities, including carbon monoxide (CO), sulfur dioxide (SO_2), and nitrogen dioxide (NO_2), were sourced from the China National Environmental Monitoring Network (http://www.cnemc.cn/en/, last access 20 August 2024). The meteorological data used in this study are listed in Table S2. These meteorological conditions are derived from the ERA5 reanalysis dataset from the European Centre for Medium-Range Weather Forecasts (ECMWF). The spatial and temporal resolutions of ERA5 data are 0.25° × 0.25° and 1 hour, respectively.

https://doi.org/10.5194/egusphere-2024-2776
Preprint. Discussion started: 25 November 2024

2.2 Measurements and inter-comparison of BC and EC

In this study, the EC data was measured using the Sunset Laboratory semi-continuous OC/EC analyzer (Model-4) with an hourly resolution. The analysis employed the National Institute for Occupational Safety and Health (NIOSH) thermal-optical transmittance (TOT) method to quantify EC. The thermal-optical approach, which forms the basis of the OC/EC analyzer, is detailed extensively in previous studies (Arhami et al., 2006; Birch & Cary, 1996; Jung et al., 2011; Zheng et al., 2014). The refractory black carbon (rBC) data from our previous work (Yang et al., 2019) was measured by a single-particle soot photometer (SP2) (Liu et al., 2010; Cross et al., 2010) for the inter-comparison between rBC and EC data. Briefly, the SP2 operates on the principle of laser-induced incandescence (LII) (Liu et al., 2010), which involves heating individual rBC particles to high temperatures using a focused laser beam. The incandescence signal emitted during the heating process is used to quantify the rBC concentration based on the characteristic heating curve of rBC particles (Liu et al., 2010).

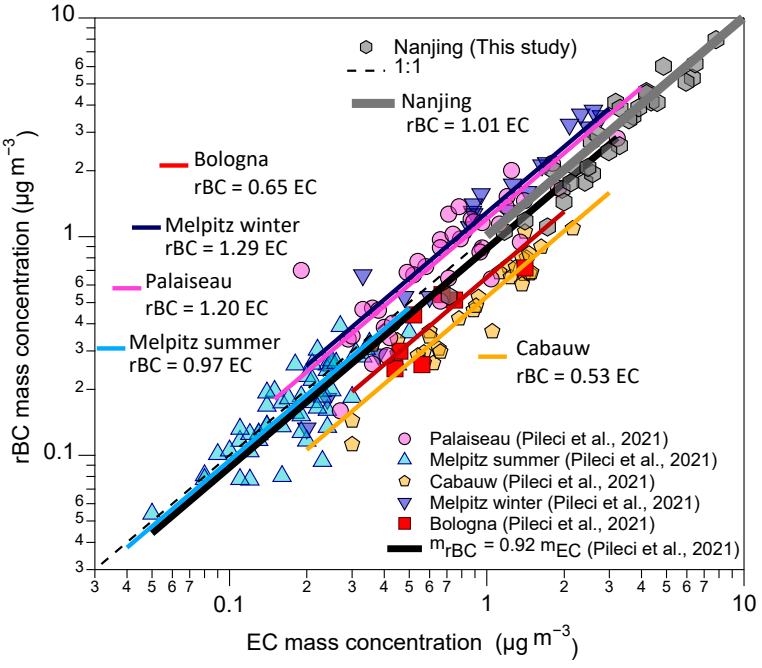

Figure 1. Comparison of rBC and EC across different regions. The rBC data for the comparison in this study was obtained from our previous work for Nanjing (Yang et al., 2019), while the comparison results in other cities were sourced from Pileci et al. (2021).

Generally, BC measurement methods could yield varying results depending on the technique used, leading to some limitations. BC measured using filter-based absorption methods is referred to as equivalent BC (eBC) (Petzold et al., 2013). This approach estimates BC content in particulate matter by measuring the light absorbed by the filter. Each of these methods carries inherent uncertainties: eBC measurements generally have an uncertainty of approximately 35% (Zanatta et al., 2016), rBC measurements around 25% (Schwarz et al., 2006), and EC measurements about 16% (Liu et al., 2013). The higher uncertainty in rBC measurements is largely attributed to the fraction of rBC mass outside the SP2 detection size range (Tinorua

https://doi.org/10.5194/egusphere-2024-2776
Preprint. Discussion started: 25 November 2024

et al., 2024). Savadkoohi et al. (2024) further underscored the importance of incorporating EC observations to reduce uncertainties inherent in eBC measurements. EC provides a more reliable representation of combustion-derived carbon components. Figure 1 presents the relationship between rBC and EC mass concentrations for datasets analyzed in this study and those from previous work (Pileci et al., 2021). The results indicate minimal bias (approximately 1%) between the rBC and EC mass concentrations on average in this study. Moreover, EC measurement methods are generally more accurate and stable, making them particularly effective in complex environments.

2.3 BC data from simulations

The Black Carbon Column Mass Density (BCC) and Black Carbon Surface Mass Concentration (BCS) data used in this study were obtained from MERRA-2 (M2T1NXADG, V5.12.4). MERRA-2 is a new reanalysis dataset released by the NASA Global Modeling and Assimilation Office (GMAO) in 2017. The spatial resolution of the data used in this study is 0.5° × 0.625°, and the temporal resolution is 1 hour. To compare with the simulated BC concentration by atmospheric chemical transport model approach, we used the Tracking Air Pollution in China (TAP) dataset (http://tapdata.org.cn/, last access 20 August 2024) (Geng et al., 2021). In brief, the TAP dataset includes the surface BC concentration data, which is simulated by the community multiscale air quality (CMAQ) model and machine learning method (Geng et al., 2021; Liu et al., 2022). BC in MERRA-2 and TAP is derived through model simulations. It is calculated based on atmospheric processes such as emission sources, chemical reactions, transport, and removal, and is therefore an output of the model (Gelaro et al., 2017; Geng et al., 2020). As a result, BC values are influenced by factors such as model assumptions, emission inventories, and meteorological conditions (Yu et al., 2024; Liu et al., 2022).

2.4 Ensemble learning models

In this study, we utilize the ensemble learning (EL) method approach to address two issues. First, we developed a model to reconstruct long-term trend of EC at urban observation sites, filling in missing data. Second, we proposed an ensemble learning approach to evaluate the driving factors of EC trends, which can quantify the contributions of emission reduction and meteorological variation to the EC trends. The two modelling methodologies integrate the predictions of Gradient Boosting Regression Trees (GBRTs), eXtreme Gradient Boosting (XGBoost), and Random Forest (RF) using ridge regression. GBRTs and XGBoost iteratively train decision tree models respectively, which reduces residuals step by step to make predictions. The final prediction results are weighted sums of the predictions from each tree model, with different weights for each tree. The RF model consists of multiple decision trees, each of which providing a prediction. The prediction method averages the results from each decision tree to obtain the prediction output, with each tree having equal weight. The final ensemble learning model, integrating the results through ridge regression to determine coefficients (m_1, m_2 and m_3) for each machine learning model, is given by Eq. 1:

$$EL = m_1\mathrm{GBRTs} + m_2\mathrm{XGBoost} + m_3\mathrm{RF}\,, \quad (1)$$

https://doi.org/10.5194/egusphere-2024-2776
Preprint. Discussion started: 25 November 2024

2.4.1 Reconstructing missing data of EC

Reconstructing long-term EC data involves integrating hourly meteorological variables and emission indicators into an ensemble learning model. Individual ensemble learning models are established for each city. As shown in Table S2, the meteorological variables include 18 factors. The emission indicators include BCC and in-situ surface observations of CO, SO_2, and NO_2. These air pollutants, along with EC, are all mainly associated with fuel combustion processes: CO concentration is closely linked to fuel combustion source activities (such as agricultural crop, forest fires and fossil fuel) (Reid et al., 2005; Wang et al., 2011). SO_2 is generally associated with industrial activities (such as coal combustion), while NO_2 primarily originates from vehicle emissions. All of them could be thereby indirectly indicating EC sources.

In our modeling approach, we used available in-situ EC observation data for each city, along with corresponding meteorological and emission indicator variables, as training and testing data set. The training data were used to establish the ensemble learning model for data reconstruction, while the testing data validated the model's performance, allowing us to determine the optimal model parameters for the best performance. All prediction parameters from 2013 to 2023 were then input into the ensemble learning model to reconstruct long-term EC data. As shown in Figure S1, the observation in Nanjing had 49161 valid data points and 92240 reconstructed data points, filling 47% of the missing data. The data completion rates for the other cities were 45% for Suzhou, 50% for Xuzhou, and 79% for Zhenjiang, respectively.

2.4.2 Quantifying drivers of EC trend with fixed emission approximation (FEA) method

The analysis of drivers behind EC trends differs from the reconstruction of missing EC data by excluding emission indicator variables from the prediction features. To quantify the factors influencing long-term reconstructed EC trends, we developed the FEA method. Using the reconstructed long-term EC data, we assume each year i (i = 2013, 2014, ..., 2023) can serve as a baseline year for the initial anthropogenic emission conditions, with data from the chosen year used to train the model. Reconstructed EC data and meteorological variables from the selected baseline year are employed as training and testing datasets to build ensemble learning models specific to individual cities. These models are subsequently applied to predict EC concentrations for the entire period from 2013 to 2023. The resulting predictions reflect variations driven solely by meteorological conditions, assuming fixed emissions at baseline-year levels. This approach effectively isolates the contributions of meteorological variations from changes driven by emissions.

The difference in the observed EC concentrations ($\Delta OBS_{(j,k)}$) between two different years (j,k) is jointly influenced by the inter-annual relative changes in EC concentrations driven by meteorological variables ($\Delta MET_{(j,k)}$) and anthropogenic emissions ($\Delta ANT_{(j,k)}$). This relationship is described mathematically in Eq. 2 as follows:

$$\Delta OBS_{(j,k)} = \Delta ANT_{(j,k)} + \Delta MET_{(j,k)}, \quad (2)$$

This equation (Eq. 2) assumes that changes in meteorology and emissions are the primary factors affecting the observed EC concentration variations between years, allowing for a decomposition of their respective contributions to the trends. The

https://doi.org/10.5194/egusphere-2024-2776
Preprint. Discussion started: 25 November 2024

$\Delta MET_{(j,k)}$ can be estimated by comparing the predicted EC concentrations for two different years ($C_{MET(i,j)}$ and $C_{MET(i,k)}$), where j and k represent the years for which predictions are made using the model trained with data from baseline year i. Specifically, j = 2013, 2014, ..., 2022, k = 2014, 2015, ..., 2023, and $k > j$). This relationship is expressed in Eq. 3, which isolates the influence of meteorological variations on inter-annual differences in EC concentrations, assuming emissions at the baseline year i level.

$$\Delta MET_{(j,k)} = C_{MET(i,k)} - C_{MET(i,j)}\ , \tag{3}$$

Thus, the impact of anthropogenic emission controls on changes in EC concentrations can be determined by subtracting $\Delta MET_{(j,k)}$, which reflects the contribution of meteorological variations, from $\Delta OBS_{(j,k)}$, the observed inter-annual EC concentration change. This relationship is expressed in Eq. 4:

$$\Delta ANT_{(j,k)} = \Delta OBS_{(j,k)} - \Delta MET_{(j,k)} \tag{4}$$

Here, $\Delta ANT_{(j,k)}$ represents the portion of the EC concentration change attributable to anthropogenic emission controls during the period between years j and k.

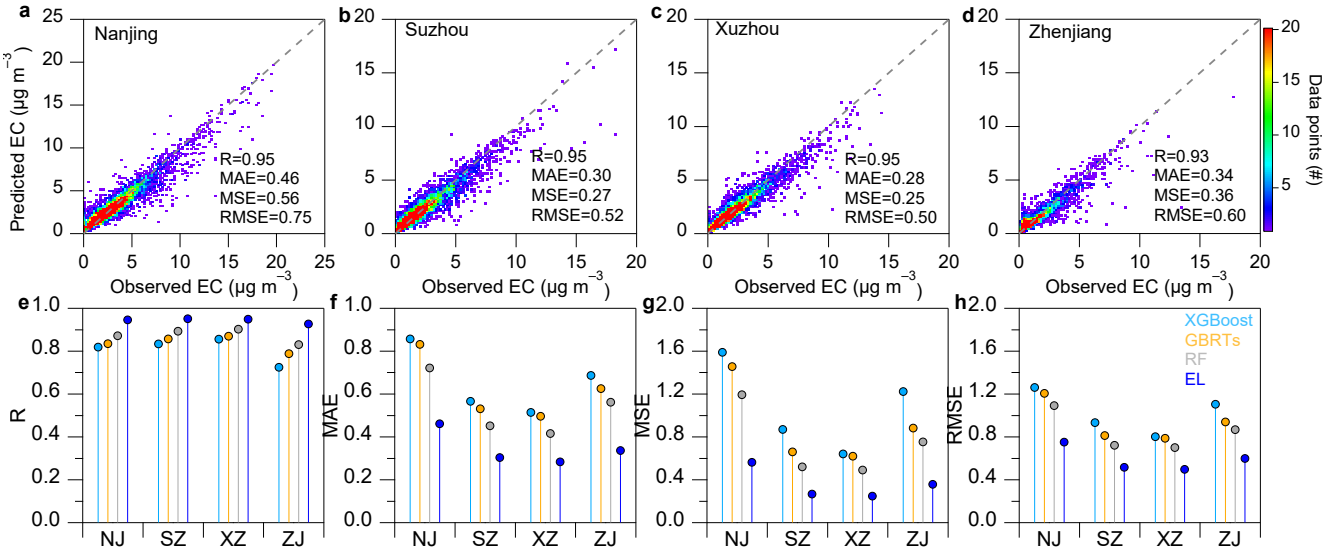

Figure 2. Performance evaluation of the models for reconstructing hourly EC concentration. **a-d** Comparison of the ensemble learning predicted concentration and observed EC concentration. The legend indicates the number of data points at each binning interval, which is approximately 0.25 μg m⁻³. **e-f** Comparison of the model performance parameters for four cities, i.e., Nanjing (NJ), Suzhou (SZ), Xuzhou (XZ), Zhenjiang (ZJ).

https://doi.org/10.5194/egusphere-2024-2776
Preprint. Discussion started: 25 November 2024

2.4.3 Model evaluation and uncertainty analysis

In this study, the errors and uncertainties of the model were assessed by comparing the reconstructed results for the test set with ground-based observational data. The statistical methods for evaluating the deviation between ground-based observed (y_{obs}) and reconstructed predicted (y_{pre}) values include root mean square error (RMSE), mean squared error (MSE), mean absolute error (MAE), and correlation coefficient (R), as shown in Eqs 5, 6, and 7:

$$\mathrm{RMSE} = \sqrt{\frac{1}{n}\sum_{i=1}^{n}\left(y_{obs} - y_{pre}\right)^2}\,, \tag{5}$$

$$\mathrm{MSE} = \frac{1}{n}\sum_{i=1}^{n}\left(y_{obs} - y_{pre}\right)^2\,, \tag{6}$$

$$\mathrm{MAE} = \frac{1}{n}\sum_{i=1}^{n}\left|y_{obs} - y_{pre}\right|\,, \tag{7}$$

To validate and assess the model's performance in reconstructing missing data, we evaluated the prediction error metrics on the test set, including RMSE, MSE, MAE, and R. Figures 2 and S2 summarize the performance metrics for individual models, including XGBoost (R=0.81±0.05), GBRTs (R=0.84±0.03), and RF (R=0.87±0.03), as well as for the ensemble learning model. The ensemble learning model exhibited a notable improvement, achieving R=0.94±0.01, which represents a 17% enhancement over the XGBoost model. Additionally, MAE, MSE, and RMSE decreased by 47%, 67%, and 42%, respectively. These findings highlight the excellent performance of the ensemble learning model compared to individual machine learning models, demonstrating its robustness and accuracy in reconstructing missing data.

To evaluate the uncertainty in the analysis of EC trend change drivers, we propose a method for quantifying the uncertainty in the FEA. The term $\Delta ANT_{(i,j)}$ is determined by subtracting $\Delta MET_{(i,j)}$ from $\Delta OBS_{(i,j)}$. By substituting Eq. 3 from the manuscript into this calculation, the relationship is expressed as shown in Eq. 8. This formulation allows for a systematic evaluation of the uncertainties associated with the FEA approach, ensuring robust attribution of trends to anthropogenic emission controls and meteorological variations. Similarly, by substituting results for the two years i and j, we can obtain $\Delta ANT_{(j,i)}$, as shown in Eq. 9.

$$\Delta ANT_{(i,j)} = \Delta OBS_{(i,j)} - \left(C_{MET(i,j)} - C_{MET(i,i)}\right)\,, \tag{8}$$

$$\Delta ANT_{(j,i)} = \Delta OBS_{(j,i)} - \left(C_{MET(j,i)} - C_{MET(j,j)}\right)\,, \tag{9}$$

If the FEA method were entirely free of uncertainty, the relationship $\left(C_{MET(i,j)} - C_{MET(i,i)}\right) + \left(C_{MET(j,i)} - C_{MET(j,j)}\right) = 0$ would hold true, implying that $\Delta ANT_{(i,j)} + \Delta ANT_{(j,i)} = 0$. However, as with any method, some degree of uncertainty is unavoidable. To account for this, the uncertainty of the data for year j, predicted using year i as the training data ($(Y_{i(j)})$, is determined by summing $\Delta ANT_{(i,j)}$ and $\Delta ANT_{(j,i)}$, and then normalizing by $C_{MET(i,j)}$. This calculation is expressed in Eq. 10:

$$Y_{i(j)} = \frac{\Delta ANT_{(i,j)} + \Delta ANT_{(j,i)}}{C_{MET(i,j)}}\,, \tag{10}$$

This approach provides a quantifiable measure of uncertainty inherent in the FEA method, facilitating a more robust evaluation of the predictions. When $i = j$, $\Delta ANT_{(i,j)} = \Delta ANT_{(j,i)} = 0$, and the uncertainty calculation at this point is expressed by Eq. 11.

https://doi.org/10.5194/egusphere-2024-2776
Preprint. Discussion started: 25 November 2024

$$Y_{i(i)} = \frac{OBS_i - C_{MET(i,i)}}{C_{MET(i,i)}}, \quad (11)$$

As shown in Figure 3, the average uncertainty across the four cities over the eleven-year period is 4 ± 4%. The lowest uncertainty is observed in Xuzhou, with 3 ± 3%, while the highest is in Suzhou, with 6 ± 5%. Based on the uncertainty metrics, we find that assuming any year as the baseline for anthropogenic emissions results in prediction errors of less than 7% for the 2013–2023 data, excluding the effects of anthropogenic emissions. However, when 2018 and 2019 are used as baseline years, the errors increase to 5.3% and 6.3%, respectively, likely due to missing meteorological parameters. For other baseline years, the errors remain below 5%. Therefore, we conclude that the attribution method used in this study is stable and reliable, and assuming year i as the baseline year for anthropogenic emissions is a reasonable approach. In Section 3.2, we will further compare the FEA method with the widely used de-weathered approach developed by Grange et al. (2018).

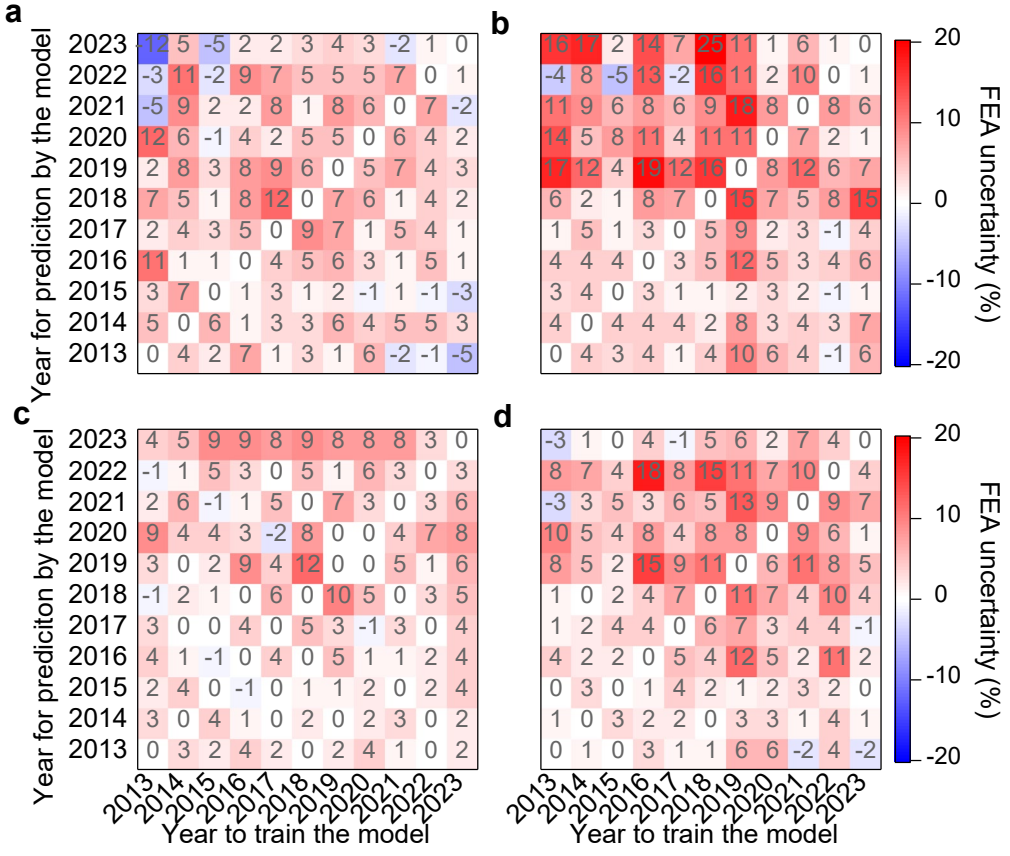

Figure 3. Cross-matrix uncertainty analysis of FEA method (a. Nanjing, b. Suzhou, c. Xuzhou, and d. Yangzhou). The uncertainty here refers to the relative difference of the results obtained from different year to train the model and different year for prediction by the model.

https://doi.org/10.5194/egusphere-2024-2776
Preprint. Discussion started: 25 November 2024

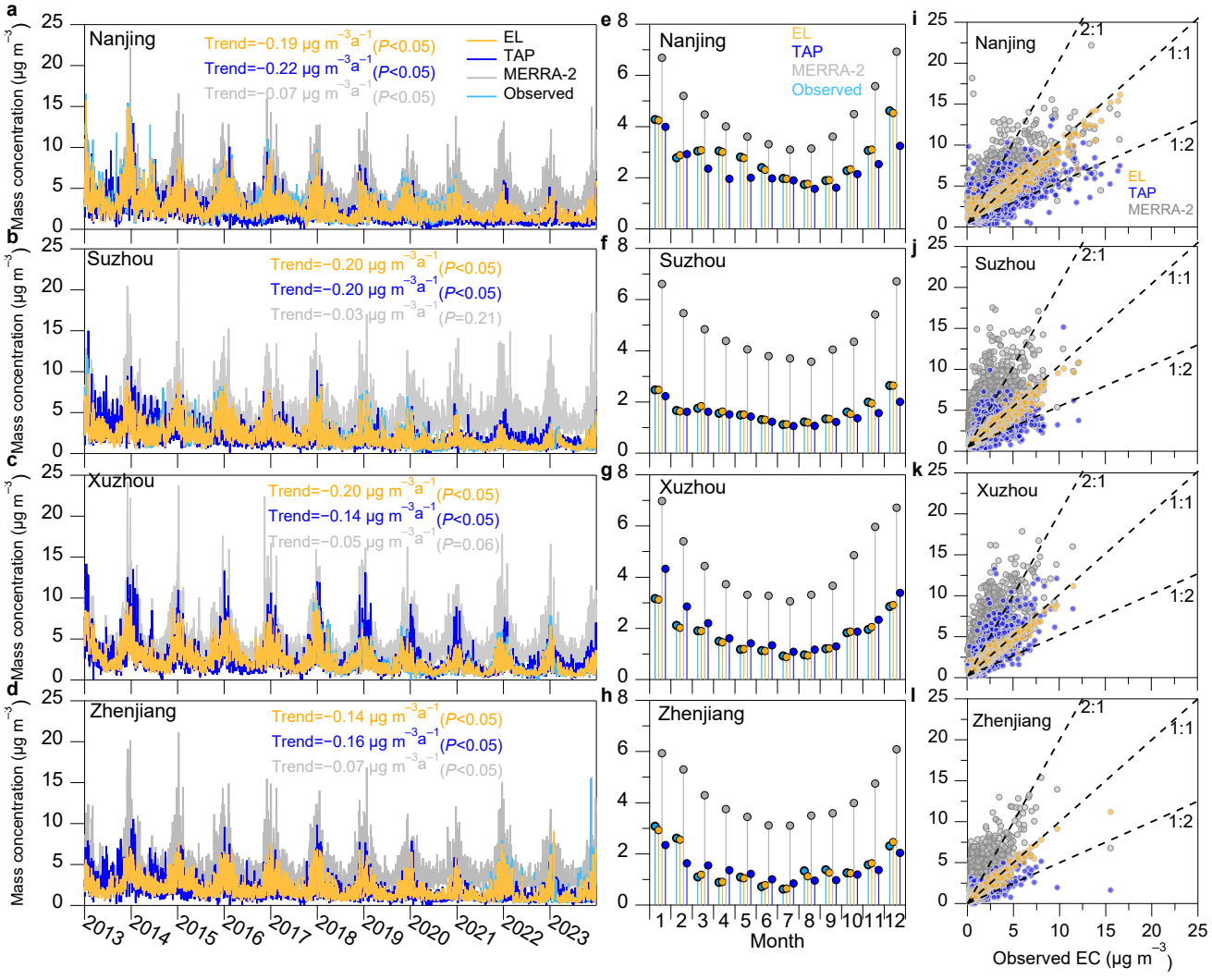

Figure 4. Comparison of EC or BC concentration from different data sets. **a-d** Trends in EC or BC concentration from the four data sets (EL, MERRA-2, TAP, and observation). **e-f** Monthly variations. **i-l** Relationship of reconstructed, MERRA-2, and TAP modeled EC or BC with observed EC.

3 Results and discussion

3.1 Reconstruction of missing data of EC and trend analysis

As shown in Figure 4a-d, the reconstructed EC concentrations in the four cities closely match the trends observed in ground-based measurements. The reconstructed EC concentrations also align well with trends from the TAP BC data, respectively. Over the 11-year period, the declining trends in reconstructed EC (-0.20 to -0.14 μg m^{-3} a^{-1}) and TAP BC (-0.22 to -0.14 μg m^{-3} a^{-1}) data are well consistent and significant ($p<0.05$). In contrast, the decline in MERRA-2 BC is less apparent,

https://doi.org/10.5194/egusphere-2024-2776
Preprint. Discussion started: 25 November 2024

particularly in Suzhou and Xuzhou, where the trend is also not statistically significant ($P > 0.05$). Additionally, MERRA-2 BC tend to overestimate EC concentrations, compared to our observations and reconstructions. Xu et al. (2020) also found similar discrepancies, noting that BC concentrations in cities like Shanghai and Hangzhou were significantly lower than that of MERRA-2. Figure 4e-h highlight that the reconstructed data exhibit excellent consistency in monthly variations with ground-based observations. This could be due to two possible reasons. First, the 0.5° × 0.625° spatial resolution of the MERRA-2 data (Randles et al., 2017), where a single grid point can cover multiple ground-based observations. Second, severe air pollution, cloud, and precipitation might impact the deviation of assimilated satellite data, which could then lead to some uncertainty of the MERRA-2 to some extent (Xu et al., 2020).

All four datasets reveal a clear seasonal pattern, with higher concentrations in autumn and winter and lower concentrations in spring and summer. These findings emphasize the importance of implementing stronger BC emission controls during the autumn and winter months. The TAP BC concentrations also show close alignment with monthly variations in ground-based data, while MERRA-2 BC overestimate the concentrations by approximately 147%. Figure 4i-l and Table S5 reveal that a moderate correlation remains ($R = 0.65 \pm 0.05$), despite MERRA-2 BC overestimating ground-based observations. The TAP BC data presents a better correlation ($R = 0.69 \pm 0.04$), compared to the MERRA-2 BC. The reconstructed data exhibit the highest correlation with ground-based observations ($R = 0.97$), indicating their high reliability during the observation period.

To evaluate the quality of the reconstructed missing data, we analyzed its correlation with co-located air pollutants (CO and NO_2), respectively. As shown in Figure S3, the observed EC concentrations exhibit good correlations with CO ($R = 0.66 \pm 0.10$) and NO_2 ($R = 0.71 \pm 0.06$) over the entire study period. Similarly, the reconstructed EC concentrations for the missing data also show good correlations with CO ($R = 0.80 \pm 0.06$) and NO_2 ($R = 0.85 \pm 0.04$) (Figure S4a-h), respectively. Additionally, the correlation between TAP BC and observation ($R = 0.65 \pm 0.05$) is better than that of MERRA-2. Figure S4 m-p indicate that the reconstructed EC for the missing data exhibits a good correlation ($R = 0.72 \pm 0.04$) with the TAP BC, with an 11% difference between the two datasets. Table S5 shows that the slope between TAP and observed EC is 0.60 ± 0.20, while the slope between TAP and reconstructed EC for the missing data is 0.68 ± 0.06. These comparisons suggest that the reconstructed data is reasonably accurate relative to ground-based observations.

Using the reconstructed EC data, we analyzed the trends of EC in four cities from 2013 to 2023. EC concentrations significantly decreased, with reductions of 61% in Nanjing and Suzhou, 59% in Xuzhou, and 47% in Zhenjiang compared to 2013 levels, respectively. In Nanjing and Xuzhou, the annual average EC concentrations decreased by 2.60 μg m^{-3} and 1.88 μg m^{-3} over the 11 years, respectively. This trend aligns with findings from Zhou et al. (2024), who reported similar decreases from 2013 to 2020 based on observational data. These reductions indicate that China's emission reduction policies have effectively mitigated BC in the Yangtze River Delta. In Suzhou and Zhenjiang, EC concentrations decreased by 1.84 μg m^{-3} and 1.17 μg m^{-3}, respectively. The average EC concentrations over the 11-year period were 2.01 ± 0.77 μg m^{-3} in Suzhou and 1.98 ± 0.50 μg m^{-3} in Zhenjiang, significantly lower than in the industrial cities of Nanjing and Xuzhou.

As shown in Figure S5a-d, the diurnal variations in EC concentrations in the four cities significantly decreased over the 11-year period, with peaks during the morning and evening rush hours primarily due to vehicle emissions. Notably, the rate of

https://doi.org/10.5194/egusphere-2024-2776
Preprint. Discussion started: 25 November 2024

EC reduction from 2020 to 2023 (-0.12 to -0.04 μg m^{-3} a^{-1}) was significantly lower than the overall rate from 2013 to 2023 (-0.20 to -0.14 μg m^{-3} a^{-1}). Zhao et al. (2024) observed a slowdown in the decline of CO/CO_2 in the Yangtze River Delta, attributing it to limited improvements in the combustion efficiency of anthropogenic sources in recent years. Figures 4a-d and S5a-d show that EC concentrations in the four cities were substantially lower during the COVID-19 pandemic from 2020 to 2022. This finding is consistent with Cui et al. (2021), who reported a significant decrease in BC concentrations during the pandemic due to lockdown measures. However, EC concentrations in Nanjing and Suzhou increased back during 2023, likely due to a rebound in anthropogenic emissions. Similarly, Liu et al. (2024) found that global carbon emissions, which temporarily decreased during the pandemic in 2021, rebounded and exceeded previous levels in 2022 and 2023. Despite significant achievements in reducing EC concentrations in the Yangtze River Delta over the past 11 years, the rate of decrease has slowed in recent years.

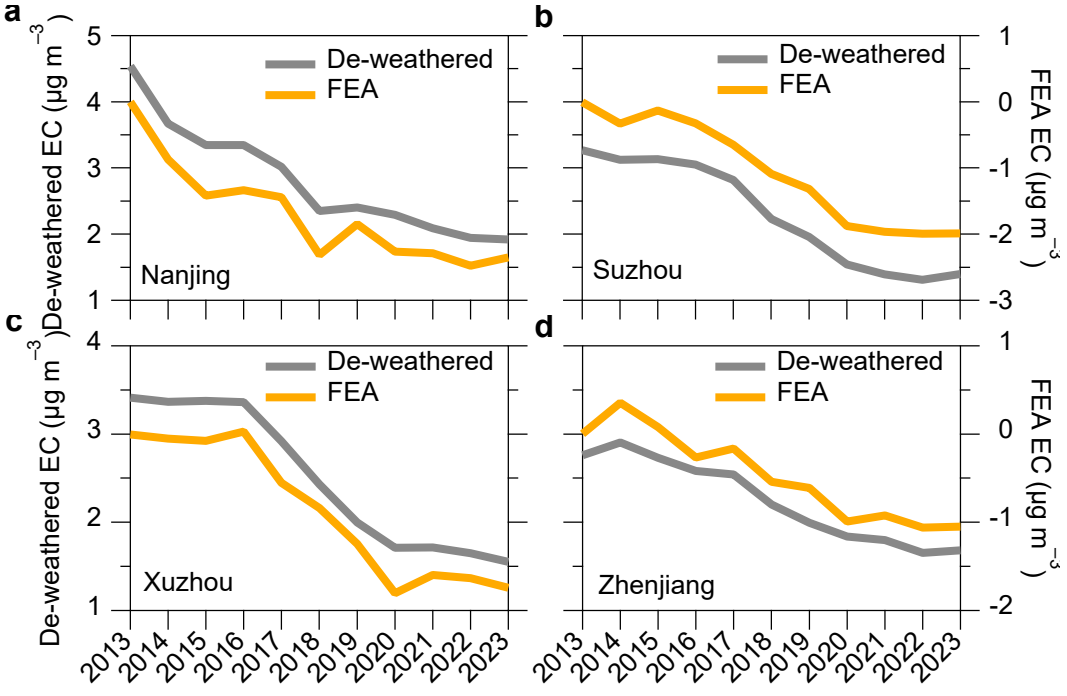

Figure 5. Trend in emission-driven EC from 2013 to 2023. Comparison of the results obtained from two different methods, including the FEA method developed in this study and the widely used de-weathered method.

3.2 Drivers of the EC trends

A new meteorological normalization method, also known as the de-weathered method (Grange et al., 2018), has been widely used to quantify the drivers of trends in air pollutants and aerosol chemical composition (Grange et al., 2018; Li et al., 2023; Vu et al., 2019; Zhang et al., 2019; Zhou et al., 2022). This method effectively separates the impacts of emissions and meteorology on these trends (Zheng et al., 2023). Detailed methodologies of this meteorological normalization can be found

https://doi.org/10.5194/egusphere-2024-2776
Preprint. Discussion started: 25 November 2024

in previous studies (e.g., Grange et al., 2018; Vu et al., 2019; Zhang et al., 2019; Zhou et al., 2022). To further compare the differences between our proposed FEA method and the traditional approach, we also quantified the emission-driven trend in EC using the meteorological normalization method. As shown in Table S6, the trends in anthropogenic emission drivers for the four cities analyzed using both methods passed the Mann-Kendall Test (P value < 0.05), with slope differences of less than 8%. The trend changes driven by anthropogenic emissions analyzed by both methods show good consistency, with differences within 10% (see Figure 5), which supports the reasonable results obtained from our proposed FEA method.

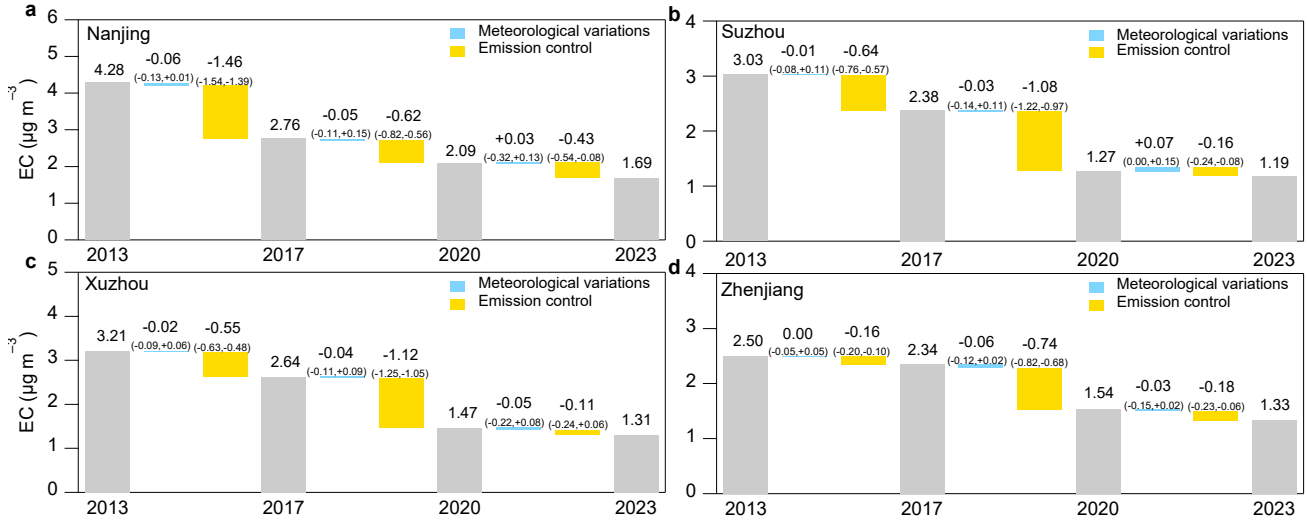

Figure 6. Drivers of the EC trend from 2013 to 2023. a-d the contributions of anthropogenic emission control and meteorological conditions on the trends in EC concentration in the four cities.

To quantify the driving factors behind EC trends – namely anthropogenic emissions and meteorology – we conducted an analysis focusing on their relative contributions. As shown in Figure S6, EC concentrations exhibited a significant downward trend from 2013 to 2023, with meteorological conditions playing a minimal role, contributing only 9±1% to the decline. In contrast, anthropogenic emission control measures accounted for 91±1% of the decrease in EC concentrations. Table S7 further illustrates that CO, SO_2, and NO_2 concentrations in the four cities from 2013 to 2023 also significant decreases, which may further support that EC trends and predominantly were driven by emission controls with negligible influence from meteorological factors. Figure S5 a-d presents the diurnal variations in EC concentrations, showing elevated levels during rush hours each year, though these peaks have notably diminished in recent years. As shown in Figure S5e-h, we also calculated the diurnal variation of emission control-driven EC relative to 2013. The results reveal that significant reductions in emission control-driven EC are associated with rush hours in urban environments. This suggests that emission control measures targeting vehicle emissions have been particularly effective in reducing EC concentrations in urban environments. This finding aligns with previous studies, such as Zheng et al. (2018), which emphasized significant reductions in BC emissions from the transportation sector in China from 2010 to 2017. Since the implementation of China's Air Pollution Prevention and Control

https://doi.org/10.5194/egusphere-2024-2776
Preprint. Discussion started: 25 November 2024

Action Plan in 2013, significant progress has been achieved in air pollution control (Zheng et al., 2018). For instance, Zhang et al. (2019) demonstrated significant decreases in $PM_{2.5}$ concentrations from 2013 to 2017, with dominant contributions from anthropogenic emission controls. To further quantify the relative contributions of different stages of emission control policies to EC concentration trends, we divided the 11-year period into three phases: 2013-2017, 2018-2020, and 2021-2023, respectively (see Figure 6).

During the implementation of China's Air Pollution Prevention and Control Action Plan, cities in the Yangtze River Delta adopted targeted strategies to mitigate BC emissions, focusing on industrial pollution control and vehicle emission standards (Zheng et al., 2018). As economically developed urban centers, Nanjing and Suzhou prioritized the management of industrial parks, while Xuzhou, a city dominated by energy production and heavy industry, emphasized reducing coal consumption and industrial emissions (Guo et al., 2022; Zhang et al., 2018). These concerted efforts significantly curbed emissions, as shown in Figure 6. Between 2013 and 2017, EC concentrations in Nanjing, Suzhou, Xuzhou, and Zhenjiang decreased by 36%, 21%, 18%, and 6%, respectively. The relatively smaller reduction in Zhenjiang could be attributed to its lower baseline EC concentration, which limited the effectiveness of emission reduction measures. Despite this, anthropogenic emissions were the predominant driver of EC concentration changes, accounting for 96%, 99%, 96%, and 98% of the observed reductions in these cities. These findings underscore the pivotal role of targeted emission control policies in achieving substantial reductions in EC pollution within the Yangtze River Delta. Following the three-year action plan from 2018 to 2020, EC reductions in Nanjing, Suzhou, Xuzhou, and Zhenjiang were 24%, 47%, 44%, and 34%, respectively. Anthropogenic emission control in Nanjing and Xuzhou significantly contributed to changes in EC concentrations, showing average reductions of -0.82 μg m^{-3} and -1.25 μg m^{-3}, respectively. These reductions were influenced by emission control measures and heightened by the substantial impact of COVID-19 lockdowns on these industrial cities in the Yangtze River Delta. Similarly, Zheng et al. (2021) observed reduced BC emissions in China during 2019-2020, particularly during the January-March lockdown, driven by abrupt emission reductions from industrial, residential, and transportation sources. The slowdown of EC concentration decline was observed during 2020-2023, with reductions of 20% (Nanjing), 7% (Suzhou), 11% (Xuzhou), and 14% (Zhenjiang), respectively. This deceleration primarily resulted from reduced contributions from anthropogenic emission controls. Figure 6 indicates that meteorological influences during this period did not significantly deviate from their overall contribution over the 11-year span. Throughout the 11 years, anthropogenic emission controls contributed to 91% of EC concentration changes, whereas during 2020-2023, these controls accounted for 93% (Nanjing), 68% (Suzhou), 67% (Xuzhou), and 86% (Zhenjiang). This suggests that China's emission reduction efforts have positively contributed to the overall decline in EC concentrations in the Yangtze River Delta. However, the efficiency of such decline has slowed in the post-pandemic years.

4 Conclusion and implication

This study presents an innovative ensemble learning approach to reconstruct hourly long-term in-situ EC data using meteorological variables and co-emitted source indicators of EC. Applied to four cities in the Yangtze River Delta of Eastern

https://doi.org/10.5194/egusphere-2024-2776
Preprint. Discussion started: 25 November 2024

China, the ensemble learning model outperformed individual algorithms such as XGBoost, GBRTs, and RF models by 17%, 13%, and 8%, respectively. The reconstructed data filled an average of 55% of the missing EC data, validated through comparisons with ground-based EC, CO, and NO_2 data, as well as TAP BC data. This method offers an efficient solution to address missing EC data in ground-based observations and helps correct uncertainties in satellite and reanalysis BC data. Over the 11-year period, EC concentrations showed an overall decline ranging from -0.20 to -0.14 $\mu g\ m^{-3}\ a^{-1}$, with a more significant decline from 2013 to 2020 (-0.24 to -0.15 $\mu g\ m^{-3}\ a^{-1}$), followed by a notable slowdown observed from 2020 to 2023 (-0.12 to -0.04 $\mu g\ m^{-3}\ a^{-1}$). We further assessed the impacts of emission reductions and meteorological conditions on EC trends using the FEA method based on the ensemble learning model as well. Anthropogenic emission controls contributed 91% to the changes in EC from 2013 to 2023, highlighting the predominant role of anthropogenic emission controls. The deceleration in EC declines from 2020 to 2023 was primarily attributable to reduced contributions from emission controls (67-93%). The ensemble learning models developed in this study provide a robust framework for reconstructing missing EC data and can be adapted to address data gaps for other air pollutants. Furthermore, the methods proposed here – ensemble learning for data reconstruction and the FEA method for trend attribution – offer promising tools for broader applications in air quality research. This study also underscores the critical role of anthropogenic emission controls in reducing urban EC concentrations in the Yangtze River Delta. To sustain and further enhance EC or BC reductions in urban environments, ongoing advancements in emission control strategies and technological innovations will be essential. These findings emphasize the importance of strengthening and optimizing policies to mitigate urban air pollution and its associated climate impacts.

Author contributions. YZ initiated and designed the study and developed the statistical methodology. YZ and QM developed the model code. QM and JF performed the simulations and analysis. YZ, SZ, YR, JQ, LT, and MZ conducted field measurements and validated the data. QM and YZ prepared the original manuscript, and XX, JP, OF, and XG provided comments on the manuscript.

Competing interests. The contact author has declared that none of the authors has any competing interests.

Acknowledgments. This study was supported by the National Natural Science Foundation of China (grant no. 42207124) and Natural Science Foundation of Jiangsu Province (grant no. BK20210663).

Data availability. The MERRA-2 (M2T1NXADG, V5.12.4) data can be downloaded at https://goldsmr4.gesdisc.eosdis.nasa.gov/data/MERRA2/M2T1NXAER.5.12.4/.
The ERA5 reanalysis data can be downloaded at https://cds.climate.copernicus.eu/cdsapp#!/dataset/reanalysis-era5-pressure-levels?tab=overview.
The TAP data is from http://tapdata.org.cn/ (Geng et al., 2021). The additional data will be made available upon request (yjzhang@nuist.edu.cn).

https://doi.org/10.5194/egusphere-2024-2776
Preprint. Discussion started: 25 November 2024

References

Arhami, M., Kuhn, T., Fine, P. M., Delfino, R. J., and Sioutas, C.: Effects of sampling artifacts and operating parameters on the performance of a semicontinuous particulate elemental carbon/organic carbon monitor, Environmental science & technology, 40, 945-954, 10.1021/es0510313, 2006.

Bali, K., Mishra, A. K., and Singh, S.: Impact of anomalous forest fire on aerosol radiative forcing and snow cover over Himalayan region, Atmospheric environment, 150, 264-275, 10.1016/j.atmosenv.2016.11.061, 2017.

Bao, F., Cheng, T., Li, Y., Gu, X., Guo, H., Wu, Y., Wang, Y., and Gao, J.: Retrieval of black carbon aerosol surface concentration using satellite remote sensing observations, Remote sensing of environment, 226, 93-108, 10.1016/j.rse.2019.03.036, 2019.

Birch, M. and Cary, R.: Elemental carbon-based method for monitoring occupational exposures to particulate diesel exhaust, Aerosol science and technology, 25, 221-241, 10.1080/02786829608965393, 1996.

Bond, T. C. and Bergstrom, R. W.: Light absorption by carbonaceous particles: An investigative review, Aerosol science and technology, 40, 27-67, 10.1080/02786820500421521, 2006.

Bond, T. C., Doherty, S. J., Fahey, D. W., Forster, P. M., Berntsen, T., DeAngelo, B. J., Flanner, M. G., Ghan, S., Kärcher, B., and Koch, D.: Bounding the role of black carbon in the climate system: A scientific assessment, Journal of geophysical research: Atmospheres, 118, 5380-5552, 10.1002/jgrd.50171, 2013.

Cross, E. S., Onasch, T. B., Ahern, A., Wrobel, W., Slowik, J. G., Olfert, J., Lack, D. A., Massoli, P., Cappa, C. D., and Schwarz, J. P.: Soot particle studies—instrument inter-comparison—project overview, Aerosol Science and Technology, 44, 592-611, 2010.

Cui, S., Xian, J., Shen, F., Zhang, L., Deng, B., Zhang, Y., and Ge, X.: One-year real-time measurement of black carbon in the rural area of Qingdao, Northeastern China: Seasonal variations, meteorological effects, and the COVID-19 case analysis, Atmosphere, 12, 394, 10.3390/atmos12030394, 2021.

Dee, D. P., Uppala, S. M., Simmons, A. J., Berrisford, P., Poli, P., Kobayashi, S., Andrae, U., Balmaseda, M., Balsamo, G., and Bauer, d. P.: The ERA-Interim reanalysis: Configuration and performance of the data assimilation system, Quarterly Journal of the royal meteorological society, 137, 553-597, 10.1002/qj.828, 2011.

Ding, A., Huang, X., Nie, W., Sun, J., Kerminen, V. M., Petäjä, T., Su, H., Cheng, Y., Yang, X. Q., and Wang, M.: Enhanced haze pollution by black carbon in megacities in China, Geophysical Research Letters, 43, 2873-2879, 10.1002/2016GL067745, 2016.

Ervens, B.: Modeling the processing of aerosol and trace gases in clouds and fogs, Chemical reviews, 115, 4157-4198, 10.1021/cr5005887, 2015.

Gelaro, R., McCarty, W., Suárez, M. J., Todling, R., Molod, A., Takacs, L., Randles, C. A., Darmenov, A., Bosilovich, M. G., and Reichle, R.: The modern-era retrospective analysis for research and applications, version 2 (MERRA-2), Journal of climate, 30, 5419-5454, 2017.

https://doi.org/10.5194/egusphere-2024-2776
Preprint. Discussion started: 25 November 2024

Geng, G., Meng, X., He, K., and Liu, Y.: Random forest models for PM2. 5 speciation concentrations using MISR fractional AODs, Environmental Research Letters, 15, 034056, 2020.

Geng, G., Xiao, Q., Liu, S., Liu, X., Cheng, J., Zheng, Y., Xue, T., Tong, D., Zheng, B., Peng, Y., Huang, X., He, K., and Zhang, Q.: Tracking Air Pollution in China: Near Real-Time PM2.5 Retrievals from Multisource Data Fusion, Environmental Science & Technology, 55, 12106-12115, 10.1021/acs.est.1c01863, 2021.

Gogoi, M. M., Babu, S. S., Imasu, R., and Hashimoto, M.: Satellite (GOSAT-2 CAI-2) retrieval and surface (ARFINET) observations of aerosol black carbon over India, Atmospheric Chemistry and Physics, 23, 8059-8079, 10.5194/acp-23-8059-2023, 2023.

Grange, S. K., Carslaw, D. C., Lewis, A. C., Boleti, E., and Hueglin, C.: Random forest meteorological normalisation models for Swiss PM 10 trend analysis, Atmospheric Chemistry and Physics, 18, 6223-6239, 10.5194/acp-18-6223-2018, 2018.

Guo, Y., Li, K., Zhao, B., Shen, J., Bloss, W. J., Azzi, M., and Zhang, Y.: Evaluating the real changes of air quality due to clean air actions using a machine learning technique: Results from 12 Chinese mega-cities during 2013-2020, Chemosphere, 300, 134608, 10.1016/j.chemosphere.2022.134608, 2022.

Harrison, R. M.: Urban atmospheric chemistry: a very special case for study, npj Climate and Atmospheric Science, 1, 20175, 10.1038/s41612-017-0010-8, 2018.

Jung, J., Kim, Y. J., Lee, K. Y., Kawamura, K., Hu, M., and Kondo, Y.: The effects of accumulated refractory particles and the peak inert mode temperature on semi-continuous organic carbon and elemental carbon measurements during the CAREBeijing 2006 campaign, Atmospheric environment, 45, 7192-7200, 10.1016/j.atmosenv.2011.09.003, 2011.

Laj, P., Lund Myhre, C., Riffault, V., Amiridis, V., Fuchs, H., Eleftheriadis, K., Petäjä, T., Salameh, T., Kivekäs, N., and Juurola, E.: Aerosol, Clouds and Trace Gases Research Infrastructure–ACTRIS, the European research infrastructure supporting atmospheric science, Bulletin of the American Meteorological Society, 10.1175/BAMS-D-23-0064.1, 2024.

Levy, R., Mattoo, S., Munchak, L., Remer, L., Sayer, A., Patadia, F., and Hsu, N.: The Collection 6 MODIS aerosol products over land and ocean, Atmospheric Measurement Techniques, 6, 2989-3034, 10.5194/amt-6-2989-2013, 2013.

Li, L., Derimian, Y., Chen, C., Zhang, X., Che, H., Schuster, G. L., Fuertes, D., Litvinov, P., Lapyonok, T., and Lopatin, A.: Climatology of aerosol component concentrations derived from multi-angular polarimetric POLDER-3 observations using GRASP algorithm, Earth System Science Data, 14, 3439-3469, 10.5194/essd-14-3439-2022, 2022.

Li, Y., Lei, L., Sun, J., Gao, Y., Wang, P., Wang, S., Zhang, Z., Du, A., Li, Z., and Wang, Z.: Significant reductions in secondary aerosols after the three-year action plan in Beijing summer, Environmental Science & Technology, 57, 15945-15955, 10.1021/acs.est.3c02417, 2023.

Liu, D., Flynn, M., Gysel, M., Targino, A., Crawford, I., Bower, K., Choularton, T., Jurányi, Z., Steinbacher, M., Hüglin, C., Curtius, J., Kampus, M., Petzold, A., Weingartner, E., Baltensperger, U., and Coe, H.: Single particle characterization of black carbon aerosols at a tropospheric alpine site in Switzerland, Atmospheric Chemistry and Physics, 10, 7389-7407, 10.5194/acp-10-7389-2010, 2010.

https://doi.org/10.5194/egusphere-2024-2776
Preprint. Discussion started: 25 November 2024

Liu, J., Bergin, M., Guo, H., King, L., Kotra, N., Edgerton, E., and Weber, R.: Size-resolved measurements of brown carbon in water and methanol extracts and estimates of their contribution to ambient fine-particle light absorption, Atmospheric Chemistry and Physics, 13, 12389-12404, 2013.

Liu, S., Geng, G., Xiao, Q., Zheng, Y., Liu, X., Cheng, J., and Zhang, Q.: Tracking Daily Concentrations of PM2.5 Chemical Composition in China since 2000, Environmental Science & Technology, 56, 16517-16527, 10.1021/acs.est.2c06510, 2022.

Liu, Z., Deng, Z., Davis, S. J., and Ciais, P.: Global carbon emissions in 2023, Nature Reviews Earth & Environment, 1-2, 10.1038/s43017-024-00532-2, 2024.

Long, C. M., Nascarella, M. A., and Valberg, P. A.: Carbon black vs. black carbon and other airborne materials containing elemental carbon: Physical and chemical distinctions, Environmental pollution, 181, 271-286, 10.1016/j.envpol.2013.06.009, 2013.

Ma, X., Yan, P., Zhao, T., Jia, X., Jiao, J., Ma, Q., Wu, D., Shu, Z., Sun, X., and Habtemicheal, B. A.: Evaluations of Surface PM10 concentration and chemical compositions in MERRA-2 aerosol reanalysis over Central and Eastern China, Remote Sensing, 13, 1317, 10.3390/rs13071317, 2021.

Matsui, H.: Black carbon absorption efficiency under preindustrial and present-day conditions simulated by a size-and mixing-state-resolved global aerosol model, Journal of Geophysical Research: Atmospheres, 125, e2019JD032316, 10.1029/2019JD032316, 2020.

Ng, N. L., Dillner, A. M., Bahreini, R., Russell, A. G., de La Beaujardière, J., Flynn, J., Gentner, D. R., Griffin, R., Hawkins, L. N., and Jimenez, J. L.: Atmospheric Science and Chemistry mEasurement NeTwork (ASCENT): A new ground-based high time-resolution air quality monitoring network, AGU Fall Meeting Abstracts, A55R-1360,

Peng, X., Liu, M., Zhang, Y., Meng, Z., Achal, V., Zhou, T., Long, L., and She, Q.: The characteristics and local-regional contributions of atmospheric black carbon over urban and suburban locations in Shanghai, China, Environmental pollution, 255, 113188, 10.1016/j.envpol.2019.113188, 2019.

Petzold, A., Ogren, J. A., Fiebig, M., Laj, P., Li, S.-M., Baltensperger, U., Holzer-Popp, T., Kinne, S., Pappalardo, G., and Sugimoto, N.: Recommendations for reporting" black carbon" measurements, Atmospheric Chemistry and Physics, 13, 8365-8379, 2013.

Pileci, R. E., Modini, R. L., Bertò, M., Yuan, J., Corbin, J. C., Marinoni, A., Henzing, B., Moerman, M. M., Putaud, J. P., and Spindler, G.: Comparison of co-located refractory black carbon (rBC) and elemental carbon (EC) mass concentration measurements during field campaigns at several European sites, Atmospheric Measurement Techniques, 14, 1379-1403, 2021.

Ramanathan, V. and Carmichael, G.: Global and regional climate changes due to black carbon, Nature Geoscience, 36, 335-358, 10.1038/ngeo156, 2008.

Randles, C., Da Silva, A., Buchard, V., Colarco, P., Darmenov, A., Govindaraju, R., Smirnov, A., Holben, B., Ferrare, R., and Hair, J.: The MERRA-2 aerosol reanalysis, 1980 onward. Part I: System description and data assimilation evaluation, Journal of climate, 30, 6823-6850, 10.1175/JCLI-D-16-0609.1, 2017.

https://doi.org/10.5194/egusphere-2024-2776
Preprint. Discussion started: 25 November 2024

Reid, J., Koppmann, R., Eck, T., and Eleuterio, D.: A review of biomass burning emissions part II: intensive physical properties of biomass burning particles, Atmospheric chemistry and physics, 5, 799-825, 10.5194/acp-5-799-2005, 2005.

Savadkoohi, M., Pandolfi, M., Favez, O., Putaud, J.-P., Eleftheriadis, K., Fiebig, M., Hopke, P. K., Laj, P., Wiedensohler, A., and Alados-Arboledas, L.: Recommendations for reporting equivalent black carbon (eBC) mass concentrations based on long-term pan-European in-situ observations, Environment international, 185, 108553, 2024.

Schwarz, J. P., Gao, R., Fahey, D., Thomson, D., Watts, L., Wilson, J., Reeves, J., Darbeheshti, M., Baumgardner, D., and Kok, G.: Single ‐ particle measurements of midlatitude black carbon and light ‐ scattering aerosols from the boundary layer to the lower stratosphere, Journal of Geophysical Research: Atmospheres, 111, 2006.

Silver, B., Reddington, C., Arnold, S., and Spracklen, D.: Substantial changes in air pollution across China during 2015–2017, Environmental Research Letters, 13, 114012, 10.1088/1748-9326/aae718, 2018.

Tinorua, S., Denjean, C., Nabat, P., Pont, V., Arnaud, M., Bourrianne, T., Dias Alves, M., and Gardrat, E.: A 2-year intercomparison of three methods for measuring black carbon concentration at a high-altitude research station in Europe, Atmospheric Measurement Techniques, 17, 3897-3915, 2024.

Valavanidis, A., Vlachogianni, T., Fiotakis, K., and Loridas, S.: Pulmonary oxidative stress, inflammation and cancer: respirable particulate matter, fibrous dusts and ozone as major causes of lung carcinogenesis through reactive oxygen species mechanisms, International journal of environmental research and public health, 10, 3886-3907, 10.3390/ijerph10093886, 2013.

Vu, T. V., Shi, Z., Cheng, J., Zhang, Q., He, K., Wang, S., and Harrison, R. M.: Assessing the impact of clean air action on air quality trends in Beijing using a machine learning technique, Atmospheric Chemistry and Physics, 19, 11303-11314, 10.5194/acp-19-11303-2019, 2019.

Wang, Q., Jacob, D. J., Fisher, J. A., Mao, J., Leibensperger, E., Carouge, C., Le Sager, P., Kondo, Y., Jimenez, J., and Cubison, M.: Sources of carbonaceous aerosols and deposited black carbon in the Arctic in winter-spring: implications for radiative forcing, Atmospheric Chemistry and Physics, 11, 12453-12473, 10.5194/acp-11-12453-2011, 2011.

Wei, C., Wang, M., Fu, Q., Dai, C., Huang, R., and Bao, Q.: Temporal characteristics and potential sources of black carbon in megacity Shanghai, China, Journal of Geophysical Research: Atmospheres, 125, e2019JD031827, 10.1029/2019JD031827, 2020.

Wei, J., Wang, J., Li, Z., Kondragunta, S., Anenberg, S., Wang, Y., Zhang, H., Diner, D., Hand, J., and Lyapustin, A.: Long-term mortality burden trends attributed to black carbon and PM2· 5 from wildfire emissions across the continental USA from 2000 to 2020: a deep learning modelling study, The Lancet Planetary Health, 7, e963-e975, 10.1016/S2542-5196(23)00235-8, 2023.

Xu, H., Ren, Y. a., Zhang, W., Meng, W., Yun, X., Yu, X., Li, J., Zhang, Y., Shen, G., and Ma, J.: Updated global black carbon emissions from 1960 to 2017: improvements, trends, and drivers, Environmental Science & Technology, 55, 7869-7879, 10.1021/acs.est.1c03117, 2021.

Xu, X., Yang, X., Zhu, B., Tang, Z., Wu, H., and Xie, L.: Characteristics of MERRA-2 black carbon variation in east China during 2000–2016, Atmospheric Environment, 222, 117140, 10.1016/j.atmosenv.2019.117140, 2020.

https://doi.org/10.5194/egusphere-2024-2776
Preprint. Discussion started: 25 November 2024

Yang, J., Ji, Z., Kang, S., and Tripathee, L.: Contribution of South Asian biomass burning to black carbon over the Tibetan Plateau and its climatic impact, Environmental Pollution, 270, 116195, 10.1016/j.envpol.2020.116195, 2021.

Yang, Y., Xu, X., Zhang, Y., Zheng, S., Wang, L., Liu, D., Gustave, W., Jiang, L., Hua, Y., and Du, S.: Seasonal size distribution and mixing state of black carbon aerosols in a polluted urban environment of the Yangtze River Delta region, China, Science of The Total Environment, 654, 300-310, 2019.

Yu, H., Li, M., Zheng, X., Zhu, M., Zheng, Z., Xie, T., Yan, G., Hu, P., Cao, Z., and Feng, J.: Potential source and health risks of black carbon based on MERRA-2 reanalysis data in a typical industrial city of North China Plain, Journal of Environmental Management, 354, 120367, 10.1016/j.jenvman.2024.120367, 2024.

Zanatta, M., Gysel, M., Bukowiecki, N., Müller, T., Weingartner, E., Areskoug, H., Fiebig, M., Yttri, K. E., Mihalopoulos, N., and Kouvarakis, G.: A European aerosol phenomenology-5: Climatology of black carbon optical properties at 9 regional background sites across Europe, Atmospheric environment, 145, 346-364, 2016.

Zhang, F., Cheng, H.-r., Wang, Z.-w., Lv, X.-p., Zhu, Z.-m., Zhang, G., and Wang, X.-m.: Fine particles (PM2. 5) at a CAWNET background site in Central China: Chemical compositions, seasonal variations and regional pollution events, Atmospheric environment, 86, 193-202, 10.1016/j.atmosenv.2013.12.008, 2014.

Zhang, S., Ren, H., Zhou, W., Yu, Y., and Chen, C.: Assessing air pollution abatement co-benefits of energy efficiency improvement in cement industry: A city level analysis, Journal of Cleaner Production, 185, 761-771, 2018.

Zhang, Y., Vu, T. V., Sun, J., He, J., Shen, X., Lin, W., Zhang, X., Zhong, J., Gao, W., and Wang, Y.: Significant changes in chemistry of fine particles in wintertime Beijing from 2007 to 2017: impact of clean air actions, Environmental Science & Technology, 54, 1344-1352, 10.1021/acs.est.9b04678, 2019.

Zhao, J., Chen, H., Qi, X., Chi, X., Jia, M., Jiang, F., Zhong, S., Zheng, B., and Ding, A.: Observed decade-long improvement of combustion efficiency in the Yangtze River Delta region in China, Environmental Research Letters, 10.1088/1748-9326/ad521e, 2024.

Zhao, J., Liu, Y., Shan, M., Liang, S., Cui, C., Chen, L., Gao, S., Mao, J., Zhang, H., and Sun, Y.: Characteristics, potential regional sources and health risk of black carbon based on ground observation and MERRA-2 reanalysis data in a coastal city, China, Atmospheric Research, 256, 105563, 10.1016/j.atmosres.2021.105563, 2021.

Zheng, B., Zhang, Q., Geng, G., Chen, C., Shi, Q., Cui, M., Lei, Y., and He, K.: Changes in China's anthropogenic emissions and air quality during the COVID-19 pandemic in 2020, Earth System Science Data, 13, 2895-2907, 10.5194/essd-13-2895-2021, 2021.

Zheng, B., Tong, D., Li, M., Liu, F., Hong, C., Geng, G., Li, H., Li, X., Peng, L., and Qi, J.: Trends in China's anthropogenic emissions since 2010 as the consequence of clean air actions, Atmospheric Chemistry and Physics, 18, 14095-14111, 10.5194/acp-18-14095-2018, 2018.

Zheng, G., Cheng, Y., He, K., Duan, F., and Ma, Y.: A newly identified calculation discrepancy of the Sunset semi-continuous carbon analyzer, Atmospheric Measurement Techniques, 7, 1969-1977, 10.5194/amt-7-1969-2014, 2014.

https://doi.org/10.5194/egusphere-2024-2776
Preprint. Discussion started: 25 November 2024

Zhou, W., Lei, L., Du, A., Zhang, Z., Li, Y., Yang, Y., Tang, G., Chen, C., Xu, W., and Sun, J.: Unexpected increases of severe haze pollution during the post COVID-19 period: Effects of emissions, meteorology, and secondary production, Journal of Geophysical Research: Atmospheres, 127, e2021JD035710, 10.1029/2021JD035710, 2022.

Zhou, Y., Zhuang, B., Wang, T., Gao, P., Li, S., Hu, Y., Li, M., Cao, H., Xie, M., and Chen, H.: Characteristics of urban black carbon aerosols in the Yangtze River Delta of China based on long-term observations, Atmospheric Environment, 326, 120488, 10.1016/j.atmosenv.2024.120488, 2024.